

A Framework for Comprehensive Impact Assessment in the Case of an Extreme Winter Scenario, Considering Integrative Aspects of Systemic Vulnerability and Resilience

**Riitta Molarius¹, Pekka Tuomaala¹, Kalevi Piira¹, Minna Räikkönen¹,
Christoph Aubrecht², Maria Polese³, Giulio Zuccaro^{3,4}, Karoliina
Pilli-Sihvola⁵ and Kalev Rannat⁶**

Abstract: In northern regions, society can be seriously interrupted by a prolonged electricity network blackout due to a winter storm that cuts off power, communication and road networks. Due to hard winter weather it is essential to enhance the resilience of society to avoid danger to life. This can be achieved by developing new models to enhance preparedness for coming disaster events and to support rescue and other authorities to focus their resources on the most vulnerable targets in actual cases of emergencies.

This paper presents a part of the results of activities performed within the EU project 'CRISMA – Modelling crisis management for improved action and preparedness'. It focuses on improved resilience by proposing a framework for systemic vulnerability and impact analyses. The described work is conceptually based on risk-hazard and socio-constructive approaches. It is illustrated by means of a scenario consisting of a prolonged blackout together with an extreme winter storm in northern Finland. Scenario components include the integrative analysis of rapidly cooling houses and exposed vulnerable people as well as estimations of the potential costs of the crisis situation. The model can be extended to handle passable routes and the deployment of available rescue and snow ploughing equipment.

Keywords: Crisis modelling, extreme winter, CRISMA, vulnerability

¹ VTT Technical Research Centre of Finland Ltd, Tampere, Finland

² AIT Austrian Institute of Technology, Energy Department, Vienna, Austria

³ University of Naples Federico II, Department of Structures for Engineering and Architecture, Naples, Italy

⁴ University of Naples Federico II, Study Centre Plinius, Naples, Italy

⁵ Finnish Meteorological Institute, Helsinki, Finland

⁶ Tallinn University of Technology, Tallinn, Estonia

1 Introduction

A prolonged electricity blackout combined with extreme winter storms may disturb society's normal life by totally disrupting human interactions. This is especially serious in sparsely populated areas where snow-blocked roads can lead to the isolation of local people and foreign visitors, and hinder rescue operations in cases of emergency. In the case of a long-lasting electricity black-out, many houses are at risk of rapid cooling and people are in danger of hypothermia.

Fallen trees, accumulated snow and high winds can damage electricity pylons and lines and block roads. When several roads get blocked at the same time across a large area, network redundancy cannot be utilized. This happened for example in January 2005 when the winter storm Gudrun left about 100,000 households without electricity in Denmark and Estonia. In addition, in Latvia approximately 400,000 and in Lithuania about 230,000 electricity customers suffered electricity cuts. In Sweden 30,000 km and in Latvia 54,000 km of power lines were damaged [Haanpää, Lehtonen, Peltonen, and Talockaite (2006)]. In Finland, a one-day storm at Christmas time 2011 cut the electricity supply to 300,000 customers. In this case the longest black-outs lasted for three weeks [Horelli (2012)]. One of the most severe situations on record with regard to cold weather-induced human mortality risk happened in 1999 in Finland when the outdoor temperature fell to -51°C , causing a power outage in Lapland due to broken cables. The situation resulted in a drop in indoor temperatures of up to 10 degrees within a few hours. Luckily, electricity was restored successfully in those hours, there was no need to evacuate anyone and no casualties were reported [Laitinen and Vainio (2009)]. In extreme winter conditions, foreign visitors may be considered even more vulnerable due to language problems as well as different safety cultures.

Systemic resilience includes the ability to prepare for and adapt to changing conditions as well as withstand and recover rapidly from disruptions [Collier, Jacobs, Saxena, Baker-Gallegos, Carroll, and Yohe (2009); Lei, Wang, Yue, Zhou, and Yin (2014)]. In the case of an extreme winter scenario, the more specific resilience of technical systems (e.g. electricity, communication and road networks) and economic systems is considered most relevant in addition to the overall resilience of societal systems (including structural prevention and rescue activities). Technical systems can only react to the imposed hazard based on their inherent features, but societal systems are also able to adjust to certain hazardous circumstances.

Community planning is a key element for building resilient societies and can be achieved by uncertainty-oriented planning. Uncertainty is caused by the lack of knowledge or distorted knowledge used in planning activities, which can be avoided or reduced by creating maps and scenarios of uncertainties of the planning area

[Jabareen (2013)]. For example, the changes in natural hazards (such as variation in snowfall, cold weather and wind storms) as well as the quality of infrastructure (e.g. buildings, roads and electricity pylons and cables) should be taken into account. To enhance the resilience of technical systems, all systems should be piloted by “safe-to-fail” design experiments, i.e. tests should be carried out to ensure that failure of the system would not have harmful effects [Lister (2007)]. One example of this kind of testing is an exercise that was done in September 2014 in Rovaniemi, Finland, where electricity companies and authorities tested their ability to quickly reconnect the city to the electricity network after a total blackout. The test pointed out some weaknesses which would impact planned actions and should be examined more closely [Fingrid (2014)].

As a kind of flipside to resilience, societal vulnerability refers to the characteristics of society making it susceptible to harmful effects of a hazard and/or associated changes which take place in the environment [Birkmann (2006); UNISDR (2009)]. From a systemic point of view, it is a multi-faceted concept that takes into account variations in demography (number of people, age classes, health status, immigration), the state of the environment (water quality, diversity, land-use, pollution), the quality of exposed assets (water and wastewater network, electricity network, transport networks, critical infrastructure), or in the working environment (economic crisis, wars etc.) for example. It is notable that both, vulnerability and resilience are in general very much context-dependent [Brooks, Adger, and Kelly (2005)].

This paper proposes a scenario-based assessment framework to investigate potential systemic impacts of an extreme winter scenario, where the electricity network is down for a prolonged period and the area under study is enduring an extreme winter storm. The paper presents a general outline and the main features of the modelling steps that are needed to simulate various aspects of the problem. Scenario-based analyses can support regional planning authorities and rescue services in preparedness planning and consequently provide crucial input for enhancing systemic resilience. After outlining the damage-oriented vulnerability assessment framework in a winter crisis scenario context, key features of the different accessible modeling tools are described. The presented approach is based on a study carried out under the umbrella of the EU-funded CRISMA project and builds upon earlier results presented by Molarius, Tuomaala, Piira, Räikkönen, Aubrecht, Polese, Zuccaro, Pilli-Sihvola, and Rannat (2014).

2 Extreme winter scenario

The hypothetical study area is located in northern Finland, with an average population density of 2 persons/km², falling to 0.2–0.5 persons/km² in rural areas. The study area, the city of Tornio, is located on the banks of the Tornionjoki and is

connected by bridge with the Swedish city of Haaparanda on the other side of the river. The scenario presents the circumstances that require strong resilience capacity from society. Resilience can be improved by using effectively several models and applications to predict possible severe situations and to prepare for them.

The chosen extreme weather scenario describes very rare circumstances where the electricity network is severely damaged for a prolonged period, lasting for days before the entire network is running again. This is combined with an extreme winter storm scenario taking place at the same time. The weather scenario (based on expert judgment, the return period is once in several hundred years) is initiated when a low-pressure system forms in southern Scandinavia in mid-December. The system moves towards Finland, bringing lots of snow which together with freezing rain causes very poor road conditions. Snow accumulation over land is 30 cm/day. The snow load starts to accumulate on trees and power lines. Already at this stage, snow ploughing capacity is at its limit and snow starts to accumulate on roads. Another low-pressure system with snow storms and winds gusting up to 24 m/s arrives a day after the first one. Two days later, a third low-pressure system hits with winds that are even stronger than before (gusts of 30–40 m/s) causing major problems on road, electricity and communication networks. Finally, the low-pressure center moves slightly southeast and cold air starts to flow from the northwest. Temperatures fall widely below -10°C . During the following 2–3 weeks, the cold weather spreads into Lapland and daytime temperatures fall widely down to between -20 and -45°C , causing a widespread need for evacuation.

3 Overall framework of the vulnerability assessment

As noted by Molarius, Tuomaala, Piira, Rääkkönen, Aubrecht, Polese, Zuccaro, Pilli-Sihvola, and Rannat (2014), the interaction of various networks (e.g. electricity, telecommunications and roads) assets (e.g. buildings) and systems (society, the economy) during bad winter circumstances is critical and must be properly considered in order to assess potential disruption. This complex situation may be studied by means of a scenario-based approach with the advantage that the scenarios can be identified by experts and, owing to the small number of scenarios, complex analysis methods of the impacts can be used [Murray, Matisziw, and Grubestic (2008)]. When a winter storm hits a region while there is a major disruption in the electricity network, a realistic scenario should consider the state of electrical, transport and communication networks, i.e. possible outages and blocked roads, the consequent cooling of houses in areas without power, the spatial location of people at risk of hypothermia or those unreachable due to blocked roads. In addition both the potential victims and the estimated scale of economic loss should be taken into account for designing impact mitigation and response measures.

The hazard intensity of a winter storm is characterized by a number of weather parameters that are variable in time and space. Therefore, the time variable and spatial extent are fundamental to impact assessment in winter scenarios. In this case study scenario, we assume that road and electricity network disruptions are determined and hence, they are not taken into account in this decision support system (see Figure 1). Instead the impact on the exposed assets and consequences in terms of potential victims and economic losses are calculated. Here, the assessment framework for estimating the potential impact of the scenario is described.

To support near real-time identification of areas affected by power outages, a satellite-based approach is presented enabling both detection of affected areas as well as monitoring gradual power recovery. In cases of extreme cold weather, the decisions can be based on two main issues: the rate of cooling of buildings and the associated human (dis)comfort. These two factors, together with the assessment of economic impacts, contribute to the determination of potential overall impact and represent the main supportive information input for decision-making in crisis response. Figure 1 illustrates the relationship of the various models and data needed for the assessment of the presented weather scenario [Molarius, Tuomaala, Piira, Rääkkönen, Aubrecht, Polese, Zuccaro, Pilli-Sihvola, and Rannat (2014)].

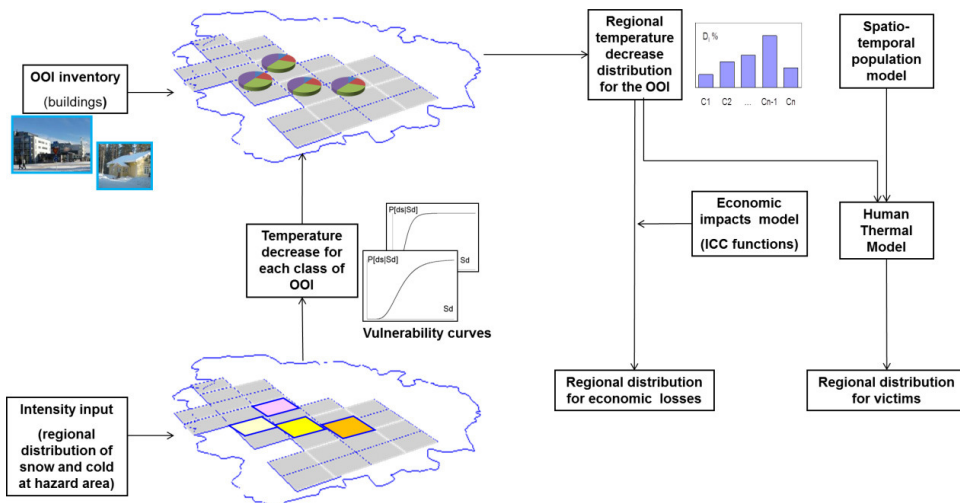


Figure 1: The relationships of the various input factors needed for simulating the consequences of an extreme cold weather scenario [Molarius, Tuomaala, Piira, Rääkkönen, Aubrecht, Polese, Zuccaro, Pilli-Sihvola, and Rannat (2014)]. OOI = Object Of Interest, ICC = Indicators, Criteria, Costs

Given the hazard intensity distribution (Intensity input), and considering available

time-dependent vulnerability curves relating the outside temperature to the temperature decrease inside buildings, it is possible to evaluate potential cooling levels in each building class at variable time steps following the outage. Knowing the inventory of the Objects of Interest (OOI), in this case buildings, it is possible to summarize each class to obtain a potential regional temperature decrease in buildings for the whole area. Combining those results with a population model, giving the distribution of people at risk, and applying a suitably developed Human Thermal Model (HTM), which estimates the state of human (dis)comfort in a cooling situation, the regional distribution of potential victims can be obtained.

4 Modeling aspects influencing systemic vulnerability and impacts of hazards

4.1 Intensity of the hazard

The intensity of the hazard is a key indicator to be used for risk and damage assessments. An illustrative way to describe the intensity of weather events is to analyze their return periods, R , i.e. the expected frequency of an event of a certain magnitude. For example, if a wind speed of 40 m/s occurs in an area once in 50 years, the return period is 50 years. Conversely, the return period can be set and the analysis results in a statistical estimate of the extreme value of the given parameter.

For this study, the extreme weather analysis was performed for minimum temperatures, maximum wind speeds, and precipitation. This was done by fitting the generalized extreme value (GEV) distribution to historical climatological data for eight weather stations in the study area. GEV is a widely used fitting method in the area of extreme value analysis [see e.g. Coles (2001); Marcelino, Villafuerte, and Matsumoto (2015)]. In addition to the maximum likelihood estimators for 50 and 100 year return periods, the 95% confidence intervals for lower and upper bounds were determined.

4.2 VTT House model and vulnerability curves

Usually, physical vulnerability functions relate the intensity of a hazard parameter to a potential damage level on a suitably established damage scale [Dolce, Masi, Marino, and Vona (2003); Schwartz and Maiwald (2012); Polese, Verderame, Mariniello, Iervolino, and Manfredi (2008); De Risi, Jalayer, De Paola, Iervolino, Giugni, Topa, Mbuya, Kyessi, Manfredi, and Gasparini (2013)]. Recently, hybrid empirical-analytical approaches were proposed for taking the damage-dependent variation of vulnerability functions into account [Polese, Marcolini, Zuccaro, and Cacace (2014a)].

Even though the cooling of houses is not strictly connected to physical damage

of buildings, it represents a serious matter for the building occupants. Thus, the vulnerability functions for buildings in case of extreme weather have been characterized in terms of indoor temperature diminution. In fact, in extreme cold weather, safety decisions in case of blackout are based on two main issues: the cooling speed of buildings, indoor temperature diminution, and the associated human comfort in respective cooling circumstances. Therefore, the estimated vulnerability functions have associated the outside temperature, which is considered as the hazard intensity parameter, to the indoor temperature after given time intervals from blackout [Polese, Zuccaro, Nardone, LaRosa, Marcolini, Coulet, Grisel, Daou, Pilli-Sihvola, Aubrecht et al. (2014b)]. The vulnerability functions were derived using a simulation-based approach; using the VTT House model for different building classes the results in terms of indoor temperature decay as a function of time from black-out were obtained, and then elaborated upon to derive suitable time-dependent vulnerability functions.

The vulnerability curves were calculated by using the online-connected VTT House building simulator for various outside temperature values. The building simulator supports cold weather-related cooling analysis of different types of buildings such as heavy apartment buildings, light single family houses, medium apartment buildings, etc. The model is based on EN ISO 13790:2008 (Energy performance of buildings: Calculation of energy use for space heating and cooling) and EN 15241:2007 (Ventilation for buildings: Calculation methods for energy losses due to ventilation and infiltration in buildings) standards as well as the models for estimating solar radiation, for example. The model includes methods for a dynamic hourly-based calculation of building energy and thermal performance, including the periods of heating and cooling, and airflow-related energy losses.

The implementation of the building model includes a web service interface, which makes it possible to use the model via the internet using third party software (Figure 2).

The input data for the model consists of buildings, weather and heating power-related information. The building information includes information available in existing building regulations, e.g. building and window type, numbers of floors, floor area, building heat capacity, window area per floor, percentage distribution of south-facing windows, air-tightness of the building envelope, ground temperature, and U-values (overall heat transfer coefficients) for base and upper floor, window and outer wall. The weather data (outside temperature, diffuse solar horizontal radiation, direct solar horizontal radiation) can be either data from a 48-hour weather forecast or locally measured data. If the local data is available, the data from the nearest weather station (latitude, longitude) is used. The required heating power input schedule is either on or off.

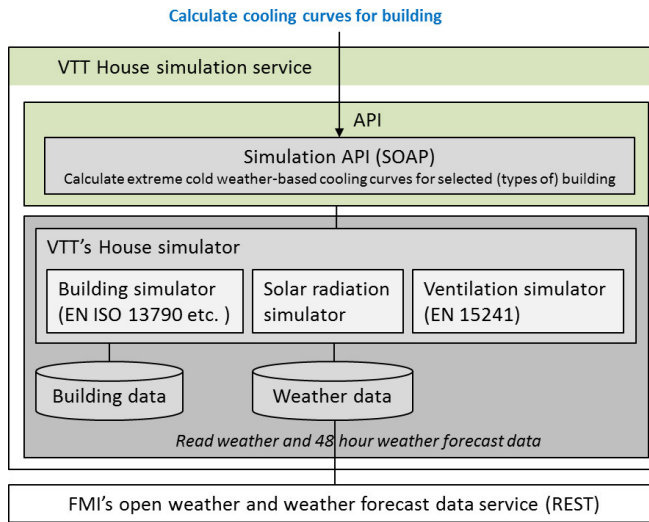


Figure 2: VTT's building simulation model for calculating extreme cold-weather related vulnerability curves

The output of the simulation model is a time series, including e.g. inside temperature and heating power. In addition to extreme weather cooling curves, the model can be used to predict the speed of temperature recovery when heating is restored.

For this study, two different building types (apartment building B1 and family house B2) with three different external envelope thermal mass levels (light L, medium M and heavy H) and seven different insulation levels (A, B, C1, C2, D1, D2, D3) were considered, and vulnerability curves obtained corresponding to increasing elapsed time from black-out.

Figure 3 shows sample simulations of the inside temperature of poorly insulated light-weight (on the left) and heavy well-insulated (on the right) apartment buildings after a power failure over 72 hours in relation to different outside temperatures.

As seen in Figure 3 the temperature drop during the first two hours is fast. This is because the used simulation model is a one-capacitance-model and the building thermal mass is connected to the middle of the external wall. This means that the initial temperature (heating on, stationary state) of that point is not the same as the indoor temperature. Hence, the hourly based calculation for the temperature drop in first two hours is not smooth. However, this is not relevant when studying cooling of the building after several hours. In heavy well-insulated buildings, the temperature decrease seems linear in time, but it appears so only because of the short time period. If we drew the cooling curves for e.g. 240 hours, the shape of the

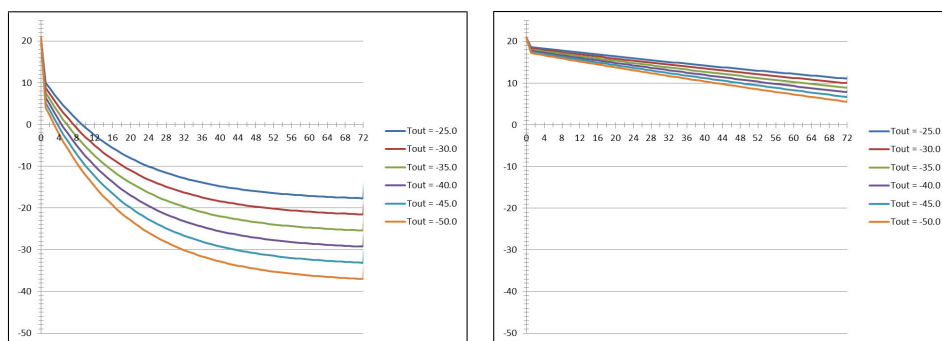


Figure 3: Development of indoor air temperature levels in poorly insulated light-weight (on the left) and heavy well-insulated (on the right) apartment buildings after a power failure ($T [^{\circ}\text{C}] = f(\text{Time} [\text{h}])$)

temperature decrease would look like that of the light-weight apartment building curves in 72 hours.

All the simulations are calculated by using fixed external temperatures. In addition the solar radiation is not included because the worst-case scenario is studied.

Figure 4 presents the vulnerability curves for an elapsed period of 24 hours for all the considered buildings, reflecting the influence of the different considered input parameters on the response of the buildings in terms of indoor cooling. These vulnerability curves are not linear for those poorly insulated light-weight apartment buildings which are by no means air tight. For this reason, the leakage air flow rate is not linearly correlated to the temperature difference between indoor and outdoor air.

The related damage probability matrices (DPMs), representing the probability of attaining different levels of indoor temperature given different outdoor temperatures and considering the inherent variability of thermal properties within each building class, may be obtained for each of the two considered building classes. Table 1 presents the DPM for building class B2 for an elapsed period of 24 hours.

The results of indoor temperature calculations support rescue services in deciding whether they have to start evacuation or whether to wait until the electricity companies are able to restore power.

The probability matrix (Table 1) is not directly a function of external temperature because the distribution of the thermal behaviour of selected apartment buildings is irregular. This means that after the selected time interval some buildings can be rather cool, some very cold, but only few buildings range between them.

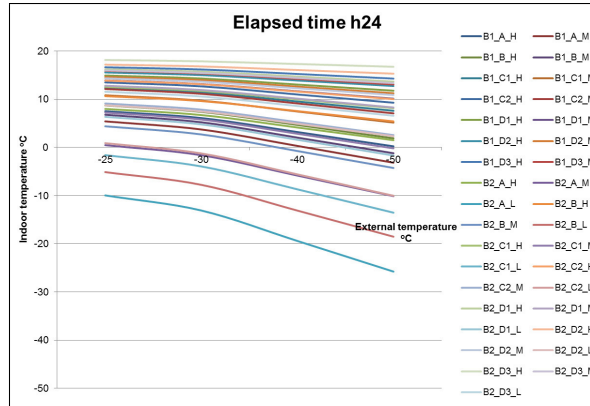


Figure 4: Vulnerability curves for an elapsed period of 24 hours [Polese, Zuccaro, Nardone, LaRosa, Marcolini, Coulet, Grisel, Daou, Pilli-Sihvola, Aubrecht et al. (2014b)]

Table 1: Damage probability matrix for elapsed time of 24 hours for building class B2 [Polese, Zuccaro, Nardone, LaRosa, Marcolini, Coulet, Grisel, Daou, Pilli-Sihvola, Aubrecht et al. (2014b)]

h24		$T_{int} [^{\circ}C]$							
$T_{ext} [^{\circ}C]$	5	0	-5	-10	-15	-20	-25	-30	-35
-25	14.3%	4.8%	9.5%	0.0%	0.0%	0.0%	0.0%	0.0%	0.0%
-30	9.5%	14.3%	4.8%	4.8%	0.0%	0.0%	0.0%	0.0%	0.0%
-40	29.0%	4.8%	14.3%	4.8%	4.8%	0.0%	0.0%	0.0%	0.0%
-50	14.3%	14.3%	0.0%	14.3%	4.8%	0.0%	4.8%	0.0%	0.0%

4.3 Building inventory and regional cooling of the buildings

The pilot building inventory consists of different types of buildings which have different heat insulation capabilities. The data for buildings is available in the Finnish Population Information System (FPIS). FPIS is a national register that contains basic information for each building all around the country, including location coordinates, gross floor area, number of floors, heating systems, year of construction, purpose of use, and number of residents.

The regional cooling model constitutes a time-dependent distribution of the number of classified buildings as a function of those buildings' cooling times in the area studied. Results of regional cooling can also be shown in terms of floor area or affected population if that information is available related to the classified building types.

For modelling, the focused region is divided into grid cells, for example of size one square kilometer each. The numbers of different classified types of building can be calculated for each grid cell. The time-dependent vulnerability curves for the classified building types are calculated starting from the results from VTT's building simulator as described above. In addition, if some high-risk buildings exist in the area, it is possible to estimate the cooling of those critical facilities at building level due to the extension options of VTT's building model.

4.4 Comparative night-time satellite image analysis

With failure of the electricity network being a major trigger to systemic risks, it is evident that rapid detection of power outages and associated causal aspects such as snow accumulation and tree fall is of utmost importance. With regard to the above-proposed assessment framework, identification of affected areas as well as monitoring of power recovery would serve as input information to pre-define priority regions where building cooling and associated impacts should be simulated.

The most rapid wide-scale option for identifying areas affected by power outages in near real-time is comparative night-time satellite image analysis, first demonstrated by Elvidge, Baugh, Hobson, Kihn, and Kroehl (1998). A standard procedure for the visual detection of power outages has been developed, based on identifying locations where lighting is usually seen to be missing or reduced following a disaster event [Aubrecht, Elvidge, Ziskin, Baugh, Tuttle, Erwin, and Kerle (2009)]. This technique can be problematic during storm conditions, as excessive cloud cover obscures lights on the Earth's surface, but it has nonetheless been successfully applied for major hurricanes and earthquakes as well as blizzards, the latter highlighting the relevance of this study. In some cases (e.g. hurricanes Wilma and Katrina in 2005), it has been possible to track the gradual recovery of power by repeating the procedure on nights following a disaster event (see Figure 5 illustrating the situation after hurricane Wilma made landfall in Western Florida on October 24, 2005).

Until recently, only the DMSP (Defense Meteorological Satellite Program) platforms' Operational Linescan System (OLS) sensor was used successfully for the detection of power outages [Elvidge, Aubrecht, Baugh, Tuttle, and Howard (2007)]. Each OLS has been capable of collecting a complete set of images of the Earth every 24 hours, with a long-term digital archive extending back to 1992. Most recently, imagery from the Visible Infrared Imaging Radiometer Suite (VIIRS) has been applied for power outage identification, e.g. during superstorm Sandy along the east coast of the United States in November 2012 as well as in California during the 2013 wildfire season. VIIRS is a sensor launched on-board the NPP platform (National Polar-orbiting Operational Environmental Satellite System Preparatory Project) in late 2011, and with its day-night band (DNB) it is supposed to pro-

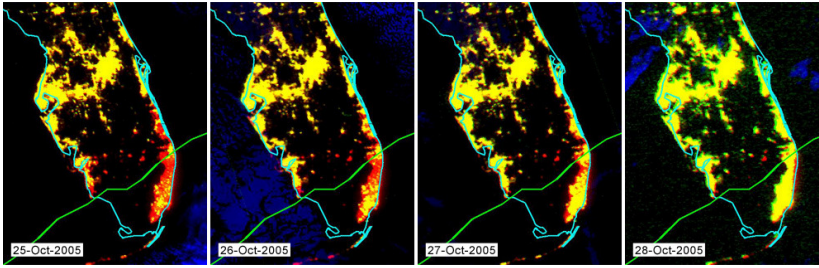


Figure 5: Detection of gradual power recovery following Hurricane Wilma affecting Miami, FL, USA, in October 2005 (red indicating power outage, yellow indicating regular lighting, green line indicating Hurricane track)

vide similar night-time detection capabilities as OLS, which is being phased out. Featuring a higher spatial resolution than OLS (approx. 750m grid cell size), VIIRS detects more structural details of the affected area, matching the level of detail of the above-described grid-level building inventory analysis. In the future, high-resolution night-time sensors may even enable local-scale analysis [Arnoux and Aubrecht (2013)].

4.5 Population Distribution Model

One of the main purposes of a spatial population distribution model in a disaster risk context is to describe where people are located at the moment of a disaster, thus assessing the potential (pre-event) or actual (during event) exposed population [Aubrecht, Özceylan, Steinnocher, and Freire (2013)]. Population distribution models can be produced at different scale levels, according to specific application needs as well as accounting for input data availability. This can range from regionally aggregated figures to very high-resolution local illustrations that go down to building level [Aubrecht, Köstl, and Steinnocher (2011)].

Due to the high granularity of the available data, a temporal dimension can be introduced into the exposure assessment [Aubrecht, Freire, Neuhold, Curtis, and Steinnocher (2012)] and, accordingly, an object-oriented spatio-temporal model can be used for implementation. In such a model, the real-world situation is approximated with the help of individual spatio-temporal atoms [Nadi and Delavar (2003)]. Real-world objects such as buildings are divided into different categories. Each category is one spatio-temporal atom, sometimes also referred to as an activity-specific disaggregation target zone. This can be a certain number of buildings associated with one activity category (e.g. residential or office buildings) or cells in a spatial grid being classified accordingly. For each atom, the population size changes individu-

ally according to time and maximum occupancy numbers can be defined.

The population estimate for a building (highest level of detail) or grid cell at a certain moment is based on time use tables that can be produced from time use surveys. As an output, the population model produces the size of the population inside the affected area at certain pre-defined time intervals. While slightly different in its general setup, in the context of possible near-continuous temporal illustration, it is in line with most recent spatio-temporal modeling developments such as *DynaPop* [Aubrecht, Steinnocher, and Huber (2014)]. Population can then be further divided into specific vulnerability groups, e.g. to account for particular disaster response measures (such as children and the elderly as well as the physically impaired, in terms of evacuation planning). However, the spatial granularity of that kind of contextual data differs and is usually coarser than the mere distributional aspects.

The main data source used by the Finnish rescue services is the FPIS which contains basic information about citizens and is maintained by the national population register center [Molarius, Korpi, Rantanen, Huovila, Yliaho, Wessberg, and Rouhainen (2009)]. This data is also available for modelling population distribution.

4.6 Human thermal model, HTM

Several simplified human thermal models are available to simulate the change of body temperature, but they are usually limited to steady-state analysis. The Human Thermal Model (HTM) has been developed to predict transient thermal behavior of a human body under changing boundary conditions, such as decreasing surrounding temperature. HTM can be used to more strictly analyze the well-being of human groups such as elderly people, children and adults inside the specified building types in order to avoid hypothermia. Since HTM estimates transient thermal interaction between an individual and surrounding space, any population can be described by giving relevant boundary conditions (e.g. gender, age, activity, and clothing insulation levels) for each occupant of interest.

HTM is based on the true anatomy and physiology of a human body, and it estimates spatial and temporal temperature levels of body tissues. For the model, the body is divided into sixteen different body parts, such as head, neck, upper arms, lower arms, hands, lower legs, etc. Each body part is further sub-divided typically into four realistic tissue layers (bone, muscle, fat, and skin) in concentric cylinders (Figure 6). Exact amounts of different tissue types at the body part level are based on typical tissue distributions given in previous studies [Smith (1991); Tuomaala (2013)], and on the individual boundary conditions presented above. Such an approach enables realistic anatomy description for any individual.

The functional tissue layers are connected to adjacent body parts by the blood circu-

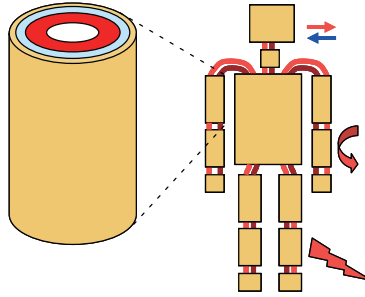


Figure 6: Anatomy model of Human Thermal Model (HTM)

lation system, which is used for physiological thermoregulation of the whole body [Holopainen (2012)]. HTM also estimates thermal interactions between the human body and the surrounding space by means of convective, radiation and evaporative heat transfer, which enables quantitative thermal sensation analysis under different boundary conditions.

When estimating human thermal sensation and thermal comfort, the influencing boundary conditions are usually divided into two groups of parameters: external and internal parameters (Figure 7). External parameters are related to the surrounding space, such as air temperature, surface temperatures, air velocity and humidity. Internal (or personal) parameters are related to the human being, i.e. clothing and metabolic rate. Furthermore, the metabolic rate depends on individual anatomy (i.e. amounts of different tissue types) and activity level.

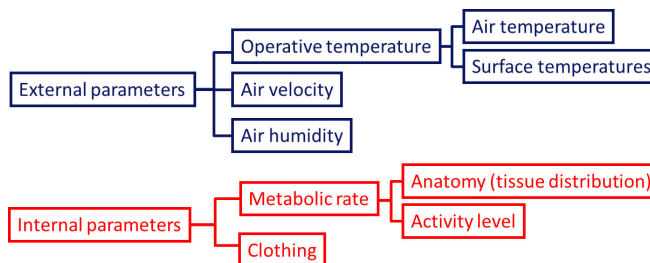


Figure 7: Space-related and occupant-related boundary conditions influencing human thermal sensation and thermal comfort

After all the impacts of both external and internal parameters on human tissue temperature levels under the desired thermal boundary conditions have been calculated, both the thermal sensation and possible level of hypothermia of an occupant can be estimated (Figure 8).

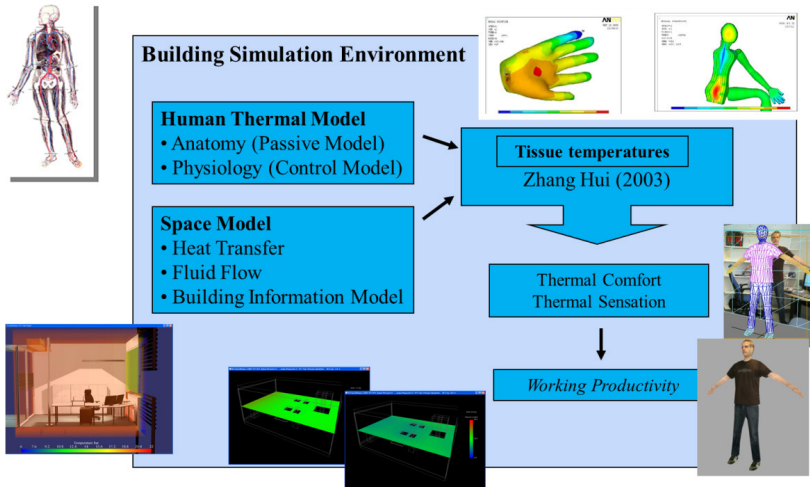


Figure 8: Simulation of tissue temperature levels, thermal sensation and comfort index values, and level of potential hypothermia of an occupant spending his/her time under studied space conditions

The local (i.e. body part level) and overall thermal sensation and thermal comfort index values are calculated using Zhang's method (2003), and the level of hypothermia can be estimated by the blood temperature leaving the heart.

One fundamental motivation for utilizing detailed HTM, instead of simplified human thermal models dealing with steady-state conditions, is the highly dynamic nature of the thermal conditions after a power failure. In addition, HTM includes features to estimate realistic physiological behavior of human bodies (e.g., reduction of blood flow in order to reduce heat losses from a body, and shivering under low temperature levels).

4.7 Dynamic Spatial Situation Assessment

Crisis management needs continuous overview of what is going on in a certain area, subarea or location. Additionally, it can be valuable for better decision making to get some estimate of crisis evolution after a fixed time-step. The Agent Models simulation tool with a dynamic map [Meriste, Helekivi, Kelder, Marandi, Motus, and Preden (2005)] is a convenient option for both. The tool offers different views to the regional or local users depending on their interests. The user has the option of visualizing several categories of concerns (Objects of Interest, OOI) in different map layers, to check their properties and follow changes over time.

Having the opportunity to use or control external models (e.g. the population mod-

el, time-dependent vulnerability model or VTT House model for critical facilities with FPIS database), it is possible to estimate the distribution of victims over a certain area. This kind of estimation, based on simulation results, serves for a better or optimal distribution of resources and helps minimize losses. From a technical point of view, each model integrated in this kind of simulation needs well-defined application programming interfaces (APIs) and internal consistency of data.

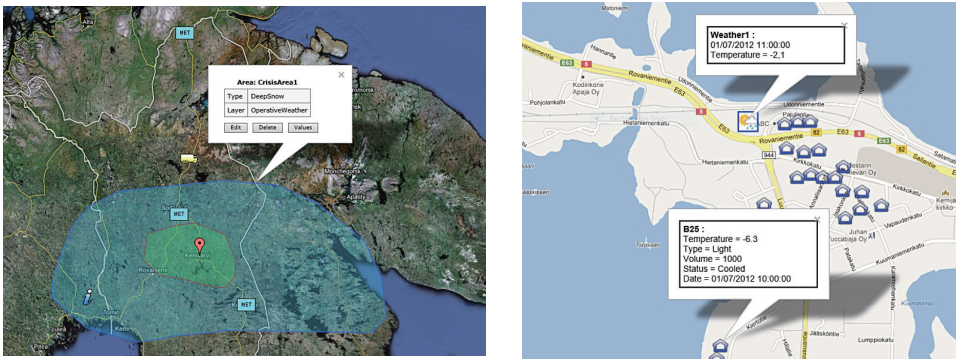


Figure 9: Large scale crisis areas (left) and a cluster of critically cooled buildings (right), visualized with DynMap

Using visualization of OOIs as seen in Figure 9, it is easy to note that the “left” option is “too generic” to decide where the local targets waiting for the intervention of rescue services might be. The “right” option becomes problematic when the number of OOIs gets large and the decision-maker loses the overview behind the details.

For the extreme winter storm case study that covers a large geographic area, there is a clear need for a new scale level in between these two options. It is convenient to divide the area of interest into 1 km² geocells. This corresponds to a choice made by Finnish emergency staff used to Finnish territorial maps and MapInfo (mapping and geographical analysis application by Pitney Bowes Software) user interface and related databases. The user can request information on almost anything situated in a numbered geocell (buildings by categories, habitants in these buildings, etc.) just by knowing the locations or other identifiers of the geocells. Naturally, the user can compile a Structured Query Language (SQL) query to get information for as many geocells as needed, which can be done after the user marks the area of interest.

The main reason for using geocells is the option of giving a more usable “general overview” in terms of where the situation is most critical with respect to certain criteria, where to allocate the resources, etc. It is nearly impossibility to lead an

operation if the number of OOIs in the target area reaches up to thousands or even tens of thousands.

The dynamic map offers the option of following the situation at geocell level and at different layers. For example, it is possible to show only the cooling status of the buildings or the situation of the inhabitants, snow and road conditions, etc. The geocell needs to have a sufficient set of properties, supporting the monitoring and visualization of all the criteria needed to support decision-making.

Like all other OOIs, the geocell in the simulation model is characterized by its properties, which describe the situation in this geocell. Among them are its ID, corner coordinates, number of inhabitants by age category, number of buildings by each category, weather conditions (mostly ambient temperature for the buildings), number of frozen buildings (temperature $< 0^{\circ}\text{C}$), and the number of people in need of evacuation.

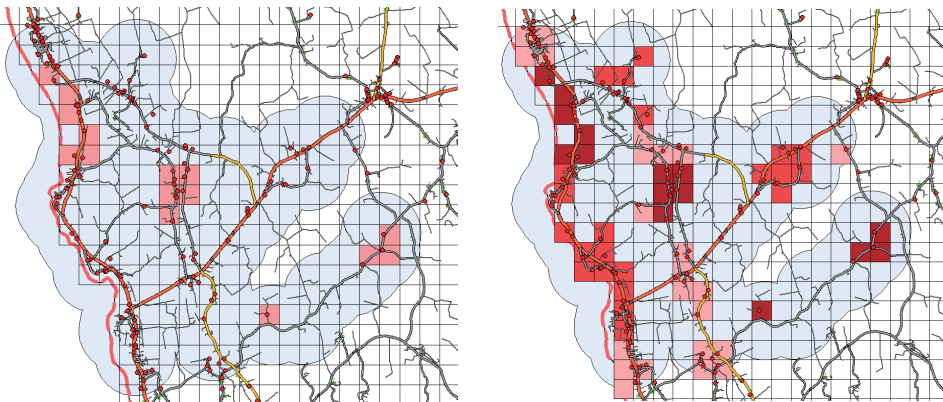


Figure 10: Simulated evolution of life condition index in geocells visualized at an intermediate time-step (left) and at the end of the simulation (right). “Light red”, “red” and “dark red” correspond to life condition indexes 0.75, 0.5 and < 0.25 accordingly.

By using geocells, the model deals with groups of people according to age categories, corresponding to different levels of vulnerability as well as groups of buildings categorized by construction and materials. For our simulation we initialized the geocells with the number of inhabitants and buildings with certain categories and types. This kind of approach gives us the possibility to follow the emergency situation from a general point of view dealing with groups of people located in numbered and geo-located geocells. It is noticed that a 1 km^2 grid is a very practical choice for both localizing the emergency and planning resource allocation.

An emergency situation in geocells is characterized by the “life condition index” as a function of the internal temperature of the buildings and the category and number of inhabitants in these buildings, calculated at each simulation time-step.

With the simulation it is easy to note how the emergency situation develops over time (Figure 10) and in which areas the “most red” cells concentrate, indicating the level of emergency by a certain criteria (for example, the number of people waiting for evacuation or the number of cooled buildings) or by a life condition index (as an integrated property of a geocell).

4.8 Economic impact of crisis, CRISECON

Extreme cold weather can and does have severe short-term economic impacts and even some longer-term consequences for economic growth. Different mitigation measures can be applied to reduce the severity of economic consequences, and preventive actions can be taken to reduce economic vulnerability and improve economic resilience.

Efficiently reducing winter risks also requires a thorough understanding of the costs of extreme winter weather. Most economic assessments of the impacts concentrate on direct losses, i.e. the financial cost of physical damage. This is mainly due to the fact that the direct losses can be quite straightforwardly evaluated monetarily, whereas indirect and intangible losses are typically more difficult to monetarize [Guha-Sapir and Hoyois (2012); Meyer, Becker, Markantonis, Schwarze et al. (2013)]. Many of the challenges related to the assessment of the economic impacts of natural disasters can be faced with the assistance of practical and systematic decision-making methods and tools.

A new economic impact approach and related software tool, CRISECON, has been developed to present impacts arising from severe winter conditions and to assess different mitigation proposals as well as the costs and benefits of alternative response strategies. Besides the quantitative assessment, the approach comprises also a semi-quantitative assessment of the economic losses. There are several methods and theories that inspired and supported the development of CRISECON: The approach for quantitative assessment is based on the methods of cost accounting and investment appraisal [Götze, Northcott, and Schuster (2008)] and the semi-quantitative assessment approach mainly follows the Analytical Hierarchy Process (AHP) [Saaty (1980)] and the methods used to estimate indirect and intangible (non-market) costs [Meyer, Becker, Markantonis, Schwarze et al. (2013)].

The main target groups for the approach and the software tool are authorities on different levels of public decision-making. In addition, the economic assessment can produce information for insurance companies, private sector investors or interna-

tional aid providers, for instance. The approach creates a common understanding of the decision alternatives and their possible consequences before the decision takes place. To meet the expert competence requirements, the analysis should be carried out in an expert session. One key for making successful decisions is the ability of the decision-maker to recognize and use external and internal sources of economic and damage information (e.g. databases, statistics, expert judgment) and to read weak signals [Räikkönen et al. (2014)].

The model uses data on alternative scenarios (e.g. base-line scenario and crisis scenario after implementing a mitigation measure) in order to make the economic assessment. The assessment is done by determining the economic losses of severe winter conditions and the costs and benefits linked to different mitigation investments and rescue strategies. The procedure mainly follows the passage from vulnerability analysis and potential damage estimation to loss assessment, focusing on discovering how such “damage” may be converted into economic losses. The basis for the assessment is a baseline scenario, which presents the simulated impacts of the winter scenario without any implemented mitigation measure(s). This baseline scenario can then be compared to a scenario including some mitigation measure(s) to evaluate the benefits, i.e. change (reduction) in damage and cost. Thus, the procedure (see Figure 11) can be applied to calculate the cost of a winter phenomenon, to determine the economic effectiveness of different mitigation investments and rescue strategies, and to compare alternative mitigation options as well as rescue strategies.

As a result of the assessment, different types of result indicators, e.g. cost summaries and graphs, can be illustrated. Effectiveness and efficiency are key outcomes in determining the best option from a set of alternatives. Typically, cost-effectiveness relates the cost of a mitigation measure to its key outcomes or benefits. The number of lives saved is an obvious unit of effectiveness.

During the CRISMA project, the approach was demonstrated and validated in a case study of a heavy winter storm in the north of Finland. The impacts arising from severe winter conditions as well as alternative mitigation proposals (e.g. a multi-hazard early warning system; the training of the emergency and rescue personnel and improved preparedness of the stakeholders involved) were assessed by applying the approach and the related software tool. Testing of the approach ensured that the necessary feedback for upgrading the approach was received. However, the depth of the research in the CRISMA project was quite limited. In the future, the approach will be tested and validated in new test cases in close cooperation with the public and private decision-makers.

The proposed approach provides a practical structure for integrating economic aspects of crises into the impact assessment and the assessment of alternative mitiga-

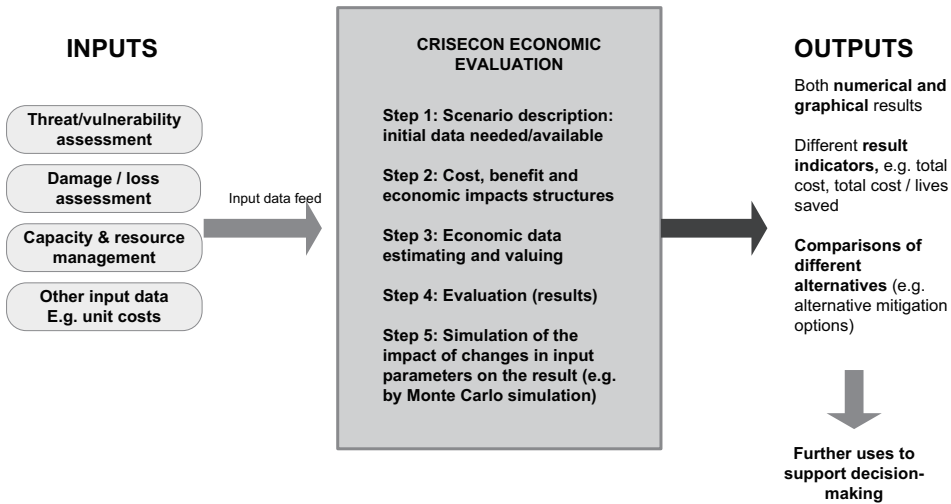


Figure 11: CRISECON model for evaluation of economic impacts (adapted from Rääkkönen et al. (2014))

tion measures. The opportunity to compare the benefits of different rescue strategies, physical investments, plans and actions enhances the transparency of decision-making and also supports long-term planning and decision-making. Furthermore, the approach contributes to the more comprehensive use of available information affecting the cost effectiveness of different mitigation investments. In all, the economic evaluation has to be flexible to handle different winter scenarios with distinct cost factors. The level of available data varies on a case-by-case basis and the assessments have to allow calculations based on detailed data as well as rough calculations with imprecise data [Rääkkönen et al. (2014)].

5 Combining the models

The main principle of performing modelling and simulation in regard to the presented models is given in Figure 12. The operator of the simulation is supported by means of planning, decision-making and data analysis. The situation analysis concept is based on comparing the changing situations during a crisis called World States (WS) as a sum of states of all individual OOIs. The evolution of the crisis is described in terms of the World States and recorded in the World State Repository (OOI-WSR).

The operator defines an initial World State (WS₀), writes it into OOI-WSR and launches the simulation for the defined number of time steps. The Agent-Oriented

Simulation Model (AOSM) reads the initial World State WS_0 from OOI-WSR and records all consecutive World States into OOI-WSR up to the end of the experiment.

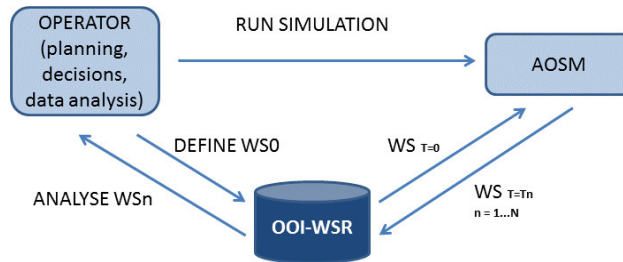


Figure 12: The main steps of the work flow for simulating the evolution of the World State (WS) of the Object of Interest (OOI): a) Define WS_0 and write it to OOI-WSR (World State Repository), b) Run simulation with AOSM (Agent Oriented Simulation Model) from $WS T = 0$ to $WS T = T_n$, $n = 1, \dots, N$, where N denotes the total number of simulation steps, c) Analyse WS_n based on data in OOI-WSR

The analysis of crisis situations is based on WS-records in OOI-WSR and performed by tools and models integrated into this application and driven over a common user interface.

The modelling and simulation application consists of the following functional blocks: Graphical User Interface (GUI), AOSM, OOI-WSR, CRISECON, Integrated Crisis Management Middleware (ICMM) and additionally, Human Thermal Model (HTM), Satellite Image Analysis, Population Distribution Model (Figure 13).

The GUI serves for general monitoring and control, OOI-WSR keeps information about the values of properties of the OOI in the different World States, AOSM offers simulation capabilities, ICMM holds metadata for simulation experiments and VTT House is used by AOSM to calculate the internal temperature for chosen categories of buildings as a function of meteorological conditions and time. CRISECON is controlled through the GUI and is used for economic cost analysis. The purpose and functionality of the Satellite Image Analyzer, Population Distribution Model and HTM was described in sections 4.4, 4.5 and 4.6.

The application provides the possibility to run several simulation scenarios (Figure 14) and to follow the changes from one WS to another. The simulation can be terminated at any time and restarted from any intermediate World State taking it as a new initial World State WS_0' for the on-going experiment.

Branching may occur at any decision point (WS) if the operator decides to change

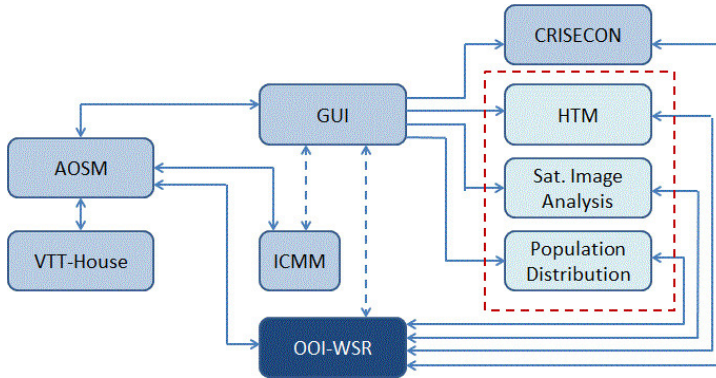


Figure 13: Functional blocks for the modelling and simulation application. The dashed line surrounding the light blue blocks denotes functional parts the integration of which is still under development. The dashed arrows denote internal functional connections for supporting simulation and World State management

some initial conditions, for example switching Power Grid ON/OFF for certain geocells or changing meteorological conditions or when the Population Distribution Model provides different data about inhabitants in a geocell. For example, at A2, A3 and B2 (Figure 14) the operator made some decisions, changed the World State and decided to test different situations evolving from these time instances (s-states) as a response to these decisions. Each time a new side branch (B, C and D) was created. This kind of experiment graph helps the operator to keep track of what is tested or simulated and to analyze the effectiveness of response actions. By analyzing the series of World States over different scenarios the operator can choose an optimal way of how and when to allocate the resources.

Decision-making concepts can be proven by running different simulation experiments and comparing the results, such as evacuation costs, between World States from different simulation scenarios or as progress over time.

6 Conclusion

One goal of the CRISMA project is to develop a framework enabling interactions both with legacy crisis management support systems and newly developed models. The accomplishment of this target has been tested in six test cases representing different kinds of hazards, among others the extreme winter weather crisis scenario described in this paper. The test results indicate that successful management of a crisis affecting a large area with several critical infrastructure networks requires the combination and interaction of various supporting models and systems.

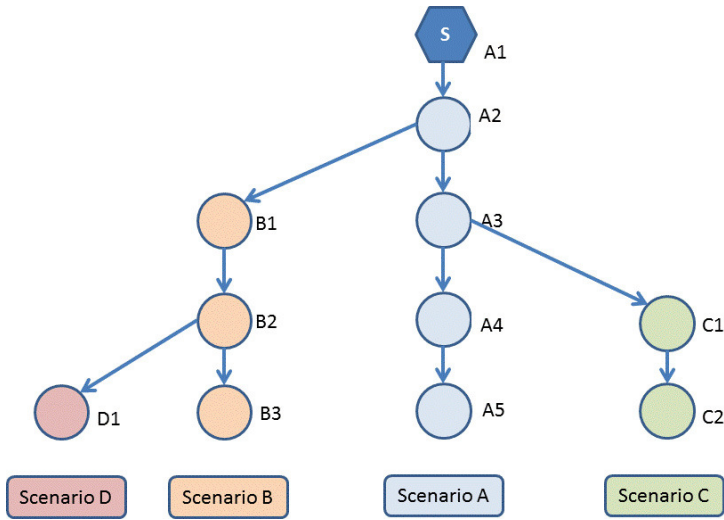


Figure 14: A fictitious scenario tree with a parent branch for scenario A, with side branches B, C and D

Wide multidisciplinary co-operation in the creation of new models and integration with legacy models, as well as making the model results visible in an effective manner is needed in order to develop a system that brings added value to decision-making in crisis management. This paper demonstrates the feasibility of both aspects, outlining the integration of new and existing models in the context of systemic vulnerability and impact assessment for the extreme winter storm scenario.

The CRISMA approach focuses on the planning phase of crisis management. Hence the developed and used models should help in decision-making to achieve better preparedness and enhance impact mitigation options for a crisis. Regional electricity outages have several negative effects on the citizen. To understand them, the rate of decrease in indoor air temperature in different types of buildings is simulated, and after that individual tissue temperature levels of citizens can be estimated. Eventually, both thermal sensations and possible levels of hypothermia among occupants can be obtained. This information can be utilized in planning evacuations or improving building regulations for buildings.

Economic assessment provides a link between the generation of proposals and an actual decision. However, there is a lack of research and appropriate tools to support cost assessments for crises, not only direct costs but also costs due to business interruption, indirect and intangible costs and mitigation costs in conditions of uncertainty. In the CRISMA project, we propose a practical model and a software

tool to show the influence of costs, risks mitigation and uncertainty aspects on crisis management decisions.

The approach and the related software tools provide a practical structure to the integration of different aspects of winter scenarios into crisis management decision-making. We believe that the developed approach fulfills its intended purpose by producing new means to support crisis management and help in rescuing vulnerable citizens in the case of winter phenomena.

Acknowledgement: This study was performed within the framework of the EU CRISMA project (www.crismaproject.eu). CRISMA is funded by the European Community's Seventh Framework Programme FP7/2007–2013 under grant agreement No. 284552. The authors would like to thank all the CRISMA colleagues for their support in producing this paper.

References

Arnoux, J.-J.; Aubrecht, C. (2013): *NYX a Night-time Optical Imaging Mission - Executive Summary*. EADS-Astrium and AIT Austrian Institute of Technology, Toulouse, France.

Aubrecht, C.; Elvidge, C.; Ziskin, D.; Baugh, K.; Tuttle, B.; Erwin, E.; Kerle, N. (2009): Observing power blackouts from space – A disaster related study. *Geophysical Research Abstracts*, vol. 11, EGU2009-7266.

Aubrecht, C.; Köstl, M.; Steinnocher, K. (2011): Population exposure and impact assessment: benefits of modeling urban land use in very high spatial and thematic detail. In: Tavares, J. M. R. S.; Natal Jorge, R. M. (Eds.): *Computational Vision and Medical Image Processing: Recent Trends. Computational Methods in Applied Sciences*, vol. 19. Dordrecht, New York: Springer, pp. 75–89.

Aubrecht, C.; Freire, S.; Neuhold, C.; Curtis, A.; Steinnocher, K. (2012): Introducing a temporal component in spatial vulnerability analysis. *Disaster Advances*, vol. 5, no. 2, pp. 48–53.

Aubrecht, C.; Özceylan, D.; Steinnocher, K.; Freire, S. (2013): Multi-level geospatial modeling of human exposure patterns and vulnerability indicators. *Natural Hazards*, vol. 68, no. 1, pp. 147–163.

Aubrecht, C.; Steinnocher, K.; Huber, H. (2014): DynaPop – population distribution dynamics as basis for social impact evaluation in crisis management. In: Hiltz, S. R.; Pfaff, M. S.; Plotnick, L.; Shih, P. C. (Eds.): *ISCRAM 2014 Conference Proceedings, 11th International Conference on Information Systems for Crisis Response and Management*. University Park, PA, USA, May, 2014, pp. 319–323.

Birkmann, J. (2006): *Measuring Vulnerability to Natural Hazards - Towards Disaster Resilient Societies*. Tokyo, New York, Paris: United Nations University Press.

Brooks, N.; Adger, W. N.; Kelly, P. M. (2005): The determinants of vulnerability and adaptive capacity at the national level and the implications for adaptation. *Global Environmental Change Part A*, vol. 15, no. 2, pp. 151–163.

Coles, S. (2001): *An Introduction to Statistical Modeling of Extreme Values*. Springer Series in Statistics, Springer, London.

Collier, W. M.; Jacobs, K.; Saxena, A.; Baker-Gallegos, J.; Carroll, M.; Yohé, G. W. (2009): Strengthening socio-ecological resilience through disaster risk reduction and climate change adaptation: Identifying gaps in an uncertain world. *Environmental Hazards*, vol. 8, no. 3, pp.171–186.

De Risi, R.; Jalayer, F.; De Paola, F.; Iervolino, I.; Giugni, M.; Topa, M. E.; Mbuya, E.; Kyessi, A.; Manfredi, G.; Gasparini, P. (2013): Flood risk assessment for informal settlements. *Natural Hazards*, vol. 69, no. 1, pp. 1003–1032.

Dolce, M.; Masi, A.; Marino, M.; Vona, M. (2003): Earthquake damage scenarios of the building stock of Potenza (Southern Italy) including site effects. *Bulletin of Earthquake Engineering*, vol. 1, no. 1, pp. 115–140.

Elvidge, C. D.; Baugh, K. E.; Hobson, V. R.; Kihn, E. A.; Kroehl, H. W. (1998): Detection of fires and power outages using DMSP-OLS data. In: Lunetta, R. S., Elvidge, C. D. (Eds.): *Remote Sensing Change Detection: Environmental Monitoring Methods and Applications*. Ann Arbor Press, pp. 123–135.

Elvidge, C. D.; Aubrecht, C.; Baugh, K.; Tuttle, B.; Howard, A. T. (2007): Satellite detection of power outages following earthquakes and other events. *3rd International Geohazards Workshop. GEO & IGOS Geohazards. Proceedings. ESA/ESRIN, Frascati (Rome), Italy*, pp. 6–9.

EN ISO 13790:2008 (2008): Energy performance of buildings – Calculation of energy use for space heating and cooling, *ISO/TC 163 and CEN/TC 89*, March 2008.

EN 15241:2007 (2007): Ventilation for buildings – Calculation methods for energy losses due to ventilation and infiltration in commercial buildings, *CEN/TC 156*, May 2007.

Fingrid (2014): The Disturbance exercise was a success and highlighted need for development. *Press Releases 9/29/2014*. Available at: <http://www.fingrid.fi/en/news/announcements/Pages/The-disturbance-exercise-was-a-success-and-highlighted-need-for-development.aspx> (accessed 11/17/2014).

Guha-Sapir, D.; Hoyois, P. (2012): *Measuring the Human and Economic Impact of Disasters*. Commissioned Review Report produced for the UK Government Office of Science, London.

Götze, U.; Northcott, D.; Schuster, P. (2008): *Investment Appraisal: Methods and Models*, Springer-Verlag: Berlin-Heidelberg.

Haanpää, S.; Lehtonen, S.; Peltonen, L.; Talockaite, E. (2006): *Impacts of Winter Storm Gudrun of 7th–9th January 2005 and Measures Taken in Baltic Sea Region*. URL: www.gsf.fi/projects/astra/sites/download/ASTRA_WSS_report_final.pdf.

Holopainen, R. (2012): *A Human Thermal Model for Improved Thermal Comfort*. VTT Science 23. Doctoral Thesis. Kuopio.

Horelli, T. (2012) *Damages in Southwestern Finland after the storm on Boxing Day 26.12.2011* (in Finnish). Report from Regional State Administrative Agency of Southwestern Finland. Publication 2:2012. Available at: <https://www.avi.fi/documents/10191/56990/Myrskyraportti+8.6.2012+LSAVI.pdf/5feb9ee3-426c-4806-99f7-220c2dd59955>. (accessed 1/12/2014).

Jabareen, Y. (2013): Planning the resilient city: Concepts and strategies for coping with climate change and environmental risk. *Cities* 2013, vol. 31, pp. 220–229.

Laitinen, J.; Vainio, S. (2009): *The Long Electricity Blackout and Securing of Critical Infrastructure* (in Finnish). Publication of the Finnish Ministry of Defence.

Lei, Y.; Wang, J.; Yue, Y.; Zhou, H.; Yin, W. (2014): Rethinking the relationships of vulnerability, resilience, and adaptation from a disaster risk perspective. *Natural Hazards*, vol. 70, no. 1, pp.609–627.

Lister, N.-M. (2007): Sustainable large parks: ecological design or designer ecology? In: Hargreaves, G., Czerniak, J. (Eds.): *Large Parks*. Architectural Press, New York / Princeton, NJ, pp. 35–54.

Meriste, M.; Helekivi, R.; Kelder, T.; Marandi, A.; Motus, L.; Preden, J. (2005): Location Awareness of Information Agents. In: Eder, J; Haav, H. M.; Kalja, A.; Penjam, J. (Eds.): *Advances in Databases and Information Systems, Proceedings: 9th East European Conference on Advances in Databases and Information Systems, ADBIS2005*. Tallinn, 12–15 September 2005. Springer, pp. 199–208.

Meyer, V.; Becker, N.; Markantonis, V.; Schwarze, R.; et al. (2013): Assessing the costs of natural hazards – state of the art and knowledge gaps. *Natural Hazards and Earth System Sciences*, vol. 13, no. 5, pp. 1351–1373.

Molarius, R.; Korpi, J.; Rantanen, H.; Huovila, H.; Yliaho, J.; Wessberg, N., and Rouhiainen, V. (2009): Assuring the information flow from accident sites to

decision makers – a Finnish case study. In: Duncan, K.; Brebbia, C. A. (Eds.): *Disaster Management and Human Health Risk – Reducing Risk, Improving Outcomes*. WIT Press, pp. 55–64.

Molarius, R.; Tuomaala, P.; Piira, K.; Räikkönen, M.; Aubrecht, C.; Polese, M.; Zuccaro, G.; Pilli-Sihvola, K.; Rannat K. (2014): Systemic vulnerability and resilience analysis regarding electricity and transport network failure in case of extreme winter storms. In: Beer, M.; Au, S.-K.; Hall, J. W. (Eds.): *Vulnerability, Uncertainty, and Risk: Quantification, Mitigation, and Management*. Reston, VA: American Society of Civil Engineers (ASCE), pp. 608–617.

Murray, A.T.; Matisziw, T.C.; Grubestic, T.H. (2008). A methodological overview of network vulnerability analysis. *Growth and Change*, vol. 39, no. 4, pp. 573–592.

Nadi, S.; Delavar, M. R. (2003): Spatio-temporal modeling of dynamic phenomena in GIS. *Proceedings of the 9th Scandinavian Research Conference on Geographical Information Science*. Espoo, Finland, pp. 247–262.

Pickands J. (1975): Statistical inference using extreme order statistics. *The Annals of Statistics*, vol. 3, no. 1, pp. 119–131.

Polese, M.; Verderame, G.M.; Mariniello, C.; Iervolino, I.; Manfredi, G. (2008): Vulnerability analysis for gravity load designed RC buildings in Naples – Italy, *Journal of Earthquake Engineering*, vol. 12, no. 2, pp. 234–245.

Polese, M.; Marcolini, M.; Zuccaro, G.; Cacace, F. (2014a): Mechanism based assessment of damaged-dependent fragility curves for RC building classes. *Bull Earthquake Engineering*, in press, doi: 10.1007/s10518-014-9663-4.

Polese, M.; Zuccaro, G.; Nardone, S.; LaRosa, S.; Marcolini, M.; Coulet, C.; Grisel, M.; Daou, M.-P.; Pilli-Sihvola, K.; Aubrecht, C.; Steinocher, K.; Humer, H.; Huber, H.; Taveter, K.; Vasiljev, S.; Reda, F.; Tuomaala, P.; Molarious, R.; Almeida, M.; Ribeiro, L. M.; Viegas, C. (2014b): *Version 2 of Dynamic Vulnerability Functions, Systemic Vulnerability, and Social Vulnerability*. Deliverable D43.2 of the Integrated project “CRISMA”, Project no. FP7/2007-2013 no. 284552, European Commission.

Saaty, T. L. (1980): *The Analytic Hierarchy Process*, McGraw-Hill, New York.

Schwartz, J.; Maiwald, H. (2012): Empirical vulnerability assessment and damage description for natural hazards following the principles of modern macroseismic scales. *Proceedings of the 15th World Conference of Earthquake Engineering*, Lisbon, Portugal.

Smith, C. (1991): *A Transient, Three-Dimensional Model of the Human Thermal System*, Doctoral Dissertation, Kansas State University, USA.

Tuomaala, P.; Holopainen, R.; Piira, K.; Airaksinen, M. (2013): Impact of individual characteristics – such as age, gender, BMI, and fitness – on human thermal sensation. *Proceedings of 13th Conference of the International Building Performance Simulation Association*. Chambéry, France. pp. 2305–2311.

UNISDR (2009): *2009 UNISDR Terminology on Disaster Risk Reduction*. Geneva, Switzerland: United Nations, May 2009.

Vajda, A.; Tuomenvirta, H.; Jokinen, P.; Luomaranta, A.; Makkonen, L.; Tikanmäki, M.; Groenemeijer, P.; Saarikivi, P.; Michaelides, S.; Papadakis, M.; Tymvios, F.; Athanasatos, S. (2011): Probabilities of adverse weather affecting transport in Europe: climatology and scenarios up to the 2050s. *Finnish Meteorological Institute Reports 2011:9*. Helsinki.

Marcelino, Q.; Villafuerte, I.; Matsumoto, J. (2015): Significant influences of global mean temperature and ENSO on extreme rainfall in southeast Asia. *J. Climate*, vol. 28, no. 5, pp. 1905–1919.

Zhang, H. (2003): *Human Thermal Sensation and Comfort in Transient and Non-uniform Thermal Environments*. Ph. D. thesis. University of California, Berkeley.